TWELFTH EUROPEAN ROTORCRAFT FORUM

Paper No 76

EXPERIENCE WITH FREQUENCY-DOMAIN METHODS IN HELICOPTER SYSTEM IDENTIFICATION

C.G. Black
D. J. Murray-Smith

Department of Aeronautics & Fluid Mechanics
and
Department of Electronics & Electrical Engineering
University of Glasgow
GLASGOW G12 8QQ, UK

G.D. Padfield

Flight Research Division
Royal Aircraft Establishment
BEDFORD MK41 6AE, UK

September 22 - 25, 1986

Garmisch-Partenkirchen

Federal Republic of Germany

Deutsche Gesellschaft für Luft- und Raumfart e. V. (DGLR)
Godesberger Allee 70, D-5300 Bonn 2, F.R.G.

EXPERIENCE WITH FREQUENCY-DOMAIN METHODS IN HELICOPTER SYSTEM IDENTIFICATION

C.G. Black
D.J. Murray-Smith

University of Glasgow

G.D. Padfield

Royal Aircraft Establishment (Bedford)

ABSTRACT

Most applications of system identification techniques to helicopters have involved time-domain methods using reduced-order mathematical models representing six-degree-of-freedom rigid-body motion. Frequency-domain techniques provide an interesting alternative approach in which data which lies outside the frequency range of interest may be disregarded. This not only provides a basis for establishing reduced order models which are valid over a defined range of frequencies but also results in a significant data reduction in comparison with time-domain methods. This paper presents a systematic approach to frequency-domain identification using both equation-error and output-error techniques. Results are presented from flight data from the Puma helicopter to illustrate the application of the frequency-domain approach to the estimation of parameters of the pitching moment and normal force equations. These results are assessed both on a statistical basis and through comparisons with theoretical values.

Nomenclature

A, B, H	state matrix, control dispersion matrix, measurement transition matrix
$\underline{b}$	vector of biases in measurements
$\underline{b}_i$	columns of matrix B in singular value decomposition
B	matrix with orthogonal columns in singular value decomposition
$\underline{f}$	function relating states to their time derivatives
$\underline{g}$	function relating states to measurements
F_{TOTAL}, F_i	total and partial F-ratios
$G(\omega)$	correction term for non-periodic window
I	identity matrix
Im	imaginary part of
j	complex number such that $j^2=-1$
J	cost function
$\underline{k}$	vector of trim constants for measurements
l_x^v, l_x^a	position relative to centre of gravity in terms of fixed body axes components (x,y,z) of measurement devices
$M_u, M_w, \ldots, M_{\eta_{1s}}$	pitching moment derivatives
N	number of samples of time-domain record
p, q, r	angular rates
$Q(s), A_z(s)$..	Laplace transformed quantities
R^2	squared correlation coefficient
Re	real part of
s	Laplace variable
s_i	singular values
S	square matrix having singular values in leading diagonal
S_v, S_α	speed and incidence angle measurement scale factors
t	time
T	record length
T_θ	time constant
u, v, w	aircraft translational velocity components
U	matrix with unit orthogonal columns used in singular value decomposition
U_e, W_e, θ_e	forward speed, normal speed and pitch angle trim components
V	orthogonal matrix used in singular value decomposition
W	diagonal weighting matrix
$\underline{x}(t), \underline{u}(t), \underline{y}(t)$	state, control and output vectors (time-domain)
$\underline{X}(\omega), \underline{U}(\omega), \underline{Y}(\omega)$	state, control and output vectors (frequency-domain)
X	matrix of independent frequency (or time) response data arranged in columns
$\underline{y}$	dependent variable - equation error method
z_{oi}, z_{ci}	observed and calculated responses
$Z_u, Z_w, \ldots, Z_{\eta_{1s}}$	normal force derivatives

β	flank angle
$\underline{\varepsilon}$	equation error term
λ	eigenvalue
θ, ϕ, ψ	Euler pitch, roll and yaw angles
$\underline{\theta}$, $\hat{\underline{\theta}}$	vector of parameters to be estimated, estimates of θ
θ_1, θ_2, etc	unknown parameters
Γ	rectangular matrix related to S
$\underline{\alpha}$	orthogonal parameter set obtained from θ
ζ	short period damping
ω, ω_{sp}	angular frequency, short period natural frequency
σ^2	residual variance
$\tau, \tau_\theta, \tau_{az}$	time delays
Ω	orthogonal matrix related to B
Δt	sampling interval
$\underline{0}$, O	null vector, null matrix
$[\ \ ]^{-1}$	inverse
$[\ \ ]^T$	transpose
exp( )	complex exponential
$\lvert\ \ \rvert$	determinant of matrix

1 INTRODUCTION

System identification techniques provide a formal mathematical basis for establishing a dynamic model of a system from measurements of its responses. This inverse modelling process involves both the identification of an appropriate model structure and the estimation of the values of parameters included within that structure. System identification and parameter estimation techniques have considerable potential in the context of helicopters, not only for the purposes of validating or improving theoretical flight mechanics models but also as an aid to flight testing of new designs.

Essential requirements of any identification technique are robustness, especially in terms of low susceptibility to noise, ease of use and clear interpretation of results through, for example, the provision of confidence intervals for estimated quantities. In any practical application of identification techniques uncertainties exist because of measurement noise, measurement offsets and process noise. Measurement noise is a term which describes errors of a random nature in the measured data whereas offsets may arise from inaccurate calibration of instruments or recording equipment. Process noise, on the other hand, arises from unmodelled features of the real system and can, for example, include effects of structural vibration associated with degrees of freedom which are not included in the model. Unexpected nonlinearities can also contribute to process noise.

Although much experience has been gained in the identification of fixed wing aircraft[1,2] far fewer successful applications have been reported in the case of rotorcraft. This relative lack of success is believed to be due to features such as the many coupled degrees of freedom in helicopters, the high vibration environment and severe limitations of test record length due to inherent instabilities.

Most published accounts of applications of system identification techniques to helicopters have been concerned with time-domain methods using a reduced-order mathematical model representing six degrees-of-freedom rigid-body motion[3-6]. The extension of such models to incorporate rotor degrees of freedom increases the system order significantly and introduces severe difficulties in terms of time-domain methods of identification. An alternative approach which may offer advantages both for the identification of six-degree-of-freedom models, and for the identification of rotor dynamics, involves the use of frequency-domain evaluation methods. In such methods the measured response data is first translated into the frequency-domain using the Fast Fourier Transformation (FFT) so that all data which lies outside the frequency range of interest may be disregarded. As well as providing a basis for developing models which are applicable over a defined range of frequencies this approach also has the advantage of reducing the amount of data required for identification. By excluding data for zero frequency the frequency-domain approach can eliminate the need to estimate the values of additive constants representing measurement zero shifts which have to be determined in the application of time-domain methods.

Interest in frequency-domain methods for aircraft parameter identification has increased during the past five years and a number of recent studies[9-12] have produced encouraging results. This paper describes aspects of a research programme involving the development and application of general-purpose software tools for frequency-domain identification of rotorcraft. This work forms part of a more broadly based programme of research, introduced in Refs. 7 and 8, which is intended to produce a complete tool-kit of robust and easily used identification techniques involving both time-domain and frequency-domain approaches.

Most of the identification techniques which have been used in recent years for the estimation of aircraft stability and control derivatives can be classified either as equation-error or output-error methods. The equation-error approach is essentially a process of ordinary-least-squares estimation carried out using data from all of the system state variables. Output-error methods, on the other hand, involve the use of an observation equation and lead to nonlinear optimisation processes[1,3].

Equation-error methods have been applied conventionally in aircraft identification using time-domain data to provide first approximations to parameter estimates which may then be used, if necessary, as initial values for output-error estimation techniques. The equation-error approach can be implemented either using a conventional least-squares algorithm, in which all of the aircraft stability derivatives are estimated simultaneously, or using step-wise regression algorithms which provide a convenient and efficient means of investigating different linear and nonlinear model structures.

It is possible to implement either a simple or stepwise regression procedure for an equation of the form

$$\underline{y} = X\,\underline{\theta} + \underline{\varepsilon} \tag{1}$$

where the vector $\underline{y}$ is formed of the estimates of the dependent variable, the matrix X involves values of the independent variables $\underline{x}_i$ arranged as columns, $\underline{\theta}$ represents the stability and control derivatives $\theta_1, \theta_2, \ldots, \theta_n$, and where the residual error $\underline{\varepsilon}(t)$ represents a combination of measurement noise on the dependent state $\underline{y}$ and any additional process noise.

The least-squares solution for the parameter vector $\underline{\theta}$ is

$$\hat{\underline{\theta}} = [\, X^T X \,]^{-1} X^T \underline{y} \tag{2}$$

These estimates of the stability and control derivatives will be unbiased only if the independent variables, $\underline{x}_i$, are free from measurement noise and any measurement noise associated with the dependent variables has zero mean. Process noise components must also have zero mean value for unbiased estimates.

For cases in which the residual vector $\underline{\varepsilon}$ is white noise the parameter covariance matrix may be written

$$\mathrm{cov}\,(\, \hat{\underline{\theta}} - \underline{\theta} \,) = \sigma^2 \,[\, X^T X \,]^{-1} \tag{3}$$

where σ^2 is the variance of the equation error.

Flight data cannot generally satisfy the above condition in terms of measurement and process noise and the residual term $\underline{\varepsilon}(t)$ may include a deterministic component. However, provided the measured response data can be filtered appropriately to eliminate noise representing unmodelled effects, useful results may be obtained by this type of method.

In the stepwise implementation of the regression process a least-squares fitting procedure is applied in a sequence of steps. At each stage independent variables are added to or deleted from the regression equation until a 'best fit' is found. The multiple correlation coefficient, R, provides a direct measure of the accuracy of fit within this process and the total F-ratio indicates the confidence associated with that fit. Partial F-ratios provide individual confidence measures for individual parameters[7].

In output-error identification a least-squares cost function is often used to provide a measure of the error between a sequence of N observed instrument readings, z_{oi}, which are corrupted by random noise, and the sequence of N calculated instrument readings z_{ci} determined from the equations of motion which have the general nonlinear form

$$\dot{x} = \underline{f}(x, t) \tag{4}$$

$$z_c = \underline{g}(x, t) \tag{5}$$

The cost function therefore has the form

$$J = \sum_{i=1}^{N} (\, z_{oi} - z_{ci})^2 \tag{6}$$

where N is the number of samples in the time-domain record. The quantities z_{ci} depend upon the values of the stability and control derivatives, the coefficients in the observation equation relating the measured output to the system states, the input time history and the initial state. Minimisation of this cost function, which is a nonlinear function of the unknown parameters, can be carried out by a number of methods such as the modified Newton-Raphson approach.

In the case of a multiple-output system it may be appropriate to multiply the sum of the squares of the fit error for each instrument by an associated weighting factor before summing to form an overall cost

$$\text{i.e.} \qquad J = \sum_{i=1}^{N} (z_{oi} - z_{ci})^T V (z_{oi} - z_{ci}) \qquad (7)$$

where V is a diagonal matrix. This forms the basis of weighted least-squares methods and represents a particular case of the more general maximum-likelihood formulation arrived at from statistical considerations[9]. Minimisation of the negative log-likelihood function results in a cost function of the form

$$J = \sum_{i=1}^{N} (z_{oi} - z_{ci})^T V (z_{oi} - z_{ci}) + \log_e |V^{-1}| \qquad (8)$$

where the weighting matrix, V, is estimated during the minimisation procedure.This is the form of cost function used for the output error results presented later in this paper.

The overall advantages of output-error methods in comparison with the equation-error approach generally are associated with the fact that output-error methods take account of noise-corrupted instrument recordings to produce unbiased estimates and, through the equations of motion, allow known relationships between parameters to be taken into account. The equation-error method does, however, provide a means of rapidly investigating questions of model structure and can provide the essential initial parameter estimates for use with the more robust output-error type methods.

3 TRANSFORMATION TO THE FREQUENCY-DOMAIN

Cost functions used for frequency-domain identification for parametric models conventionally involve a summation of frequency-dependent values. If all the values obtained from the application of the FFT to the measured response data were used in the estimation process there would be a direct equivalence, by Parseval's Theorem, between the cost functions in the time-domain and their frequency-domain counterparts[9]. The time-domain and frequency-domain approaches are, however, no longer equivalent if the frequencies included in the cost function are restricted to include only those values within a given range. This selective process in the frequency-domain is, of course, equivalent to time-domain estimation after filtering to remove unwanted components but is computationally simpler in that it avoids the need to create a new data set for each different filter time constant.

Figures 1 and 2 show typical flight data records obtained using the RAE research Puma helicopter, a brief description of which may be found in Refs. 7 and 8. Records are shown for two cases which also provide the basis of the applications presented in later sections of the paper. The first of these two records, which involve representations both in the time-domain and in the frequency-domain, illustrates the Puma response to a longitudinal cyclic doublet input at 100 knots while the second shows the response to a DFVLR '3211' longitudinal cyclic test input, again at 100 knots. The upper limit of frequency (0.56 Hz.) used in the identification studies is shown and reconstructed time-domain records, determined from the truncated frequency-domain data sets using only eight frequencies, are superimposed upon the original time histories. These reconstructed records show very clearly that the higher frequencies have been filtered out by this truncation process. Figure 3 provides an illustration of the effect of using different frequency ranges in this reconstruction process and demonstrates clearly the degree of filtering achieved as the cut-off frequency is reduced.

Although the main justification for introducing selectivity in the frequencies used for identification is connected with the need to obtain models which are valid for a specified frequency range, the resultant data reduction is also beneficial in computational terms. The availability of frequency-domain records also provides a very useful indication of the degree of excitation of the system at frequencies of interest.

One problem in the application of frequency-domain methods to helicopter parameter estimation is that the measured quantities, and the quantities used in a state space description of the system are not,in general, related linearly. Practical difficulties are encountered in applying linear transformations, such as the discrete Fourier transformation, to nonlinear equations of the form of (4) and (5), and linearisation is therefore necessary. Measurement offsets relative to the centre of gravity also have to be taken into consideration in this context.

A general linearised model, valid for a given flight condition and small amplitude excursions, can be written in the form

$$\dot{\mathbf{x}}(t) = A\,\mathbf{x}(t) + B\,\mathbf{u}(t) \tag{9}$$

$$\mathbf{y}(t) = H\,\mathbf{x}(t) + \mathbf{k} + \mathbf{b} \tag{10}$$

where A and B represent the stability and control derivatives respectively, H is a matrix relating model outputs $\mathbf{y}$ to the state variables $\mathbf{x}$, $\mathbf{k}$ is a vector of trim constants and $\mathbf{b}$ is a constant vector of biases. Transformation to the frequency-domain gives

$$\dot{\mathbf{X}}(\omega) = A\,\mathbf{X}(\omega) + B\,\mathbf{U}(\omega) \tag{11}$$

$$\mathbf{Y}(\omega) = H\,\mathbf{X}(\omega) \qquad \omega \neq 0 \tag{12}$$

Using the relationship between the Fourier transform of a variable and the Fourier transform of the time derivative of that variable, it is possible to write

$$\dot{\mathbf{Y}}(\omega) = j\omega\,\mathbf{Y}(\omega) + \mathbf{G}(\omega) \tag{13}$$

where

$$G(\omega) = \frac{\sqrt{N}}{T}\left[\mathbf{y}\left(T - \frac{\Delta t}{2}\right) - \mathbf{y}\left(-\frac{\Delta t}{2}\right)\right]\exp\left(\frac{j\omega\Delta t}{2}\right) \tag{14}$$

and where N is the number of samples in the time-domain record, Δt is the sampling interval and T is the record length in seconds. The term $\mathbf{G}(\omega)$ arises from the integration involved in the Fourier transformation of $\dot{\mathbf{x}}(t)$ in equation (9)[11]. The terms $\mathbf{y}(T - \frac{\Delta t}{2})$ and $\mathbf{y}(-\frac{\Delta t}{2})$ are obtained by linear interpolation using two points not employed in the estimation. The quantity $G(\omega)$ exists for all cases involving non-periodic windows and is given here in terms of the definition of the discrete Fourier transform used in the NAG library of computer subroutines[14]. Such cases are the norm for flight data since the values of output variables are seldom the same at the beginning and end of each test record (i.e. $\mathbf{y}(0) \neq \mathbf{y}(T)$)[11]. The model may therefore be represented in the frequency-domain by the equations

$$\dot{\mathbf{Y}}(\omega) = j\omega\,\mathbf{Y}(\omega) + \mathbf{G}(\omega) = H\,\dot{\mathbf{X}}(\omega) \tag{15}$$

so that

$$j\omega\,\mathbf{Y}(\omega) = H\,A\,\mathbf{X}(\omega) + H\,B\,\mathbf{U}(\omega) - \mathbf{G}(\omega) \tag{16}$$

The frequency-domain quantities $\mathbf{X}(\omega)$ and $\dot{\mathbf{X}}(\omega)$ which appear in equation (11) may therefore be obtained from knowledge of $\mathbf{Y}(\omega)$ and $\mathbf{G}(\omega)$ using equations (15) and (16).

These equations thus provide an alternative to the use of the Extended Kalman Filter/Smoother[15] in constructing time-domain and frequency-domain records of unmeasured states as a preliminary to the application of parameter estimation techniques. For example, states in the model and the measured quantities are directly related by equation (12) and so the frequency-domain records $\mathbf{X}(\omega)$ may be obtained by directly transforming the raw flight data and effectively solving this equation for the small number of points normally used for frequency-domain estimation. With the output error type of approach elements of the measurement transition matrix H themselves may be included among the parameters for which estimates are sought. It must be recognised, however, that the Extended Kalman Filter/Smoother produces minimum variance estimates of the system states and that it can also provide a basis for valuable kinematic consistency checks[7]. The Extended Kalman Filter/Smoother state estimation of the flight data does have a disadvantage in that the somewhat subjective and difficult selection of process noise statistics has to be made. The frequency-domain approach of equations (15) and (16) does not eliminate the need for state estimation based upon Kalman filtering but provides an interesting alternative tool which can be applied with advantage in certain cases.

4 EQUATION ERROR METHODS IN THE FREQUENCY-DOMAIN

Frequency-domain data can be used to obtain a model of the form of equations (11) and (12) using either the least-squares solution (equations (2) and (3)) or the stepwise regression procedure where state variables are introduced to, or removed from, the model on the basis of statistical significance tests. The frequency range over which data is used in the parameter estimation process, and consequently for which the estimated model is valid, must be selected on the basis of the intended application of the model. An appropriate frequency range can often be chosen by inspection of plots (e.g. Fig. 1) indicating the magnitude of transformed pairs at each frequency.

In practical terms, the evaluation of the cost function in the frequency-domain involves both real and imaginary components at each frequency used. The process implemented in the work reported here is based upon a cost function involving a Euclidean norm formed from elements representing the complex valued equation error terms which follow from transformation of equation (1). This cost function may be expressed in the following form

$$J = \sum_{\omega_1}^{\omega_2} \left[\{Re[\varepsilon(\omega)]\}^T\{Re[\varepsilon(\omega)]\} + \{Im[\varepsilon(\omega)]\}^T\{Im[\varepsilon(\omega)]\} \right] \qquad (17)$$

One of the fundamental problems of helicopter parameter identification is associated with the breakdown in the confidence in the estimates of certain parameters when there are significant correlations between pitch, roll and yaw rates[8]. A possible approach which may lead to successful results in such cases involves rank-deficient solutions[16] in which small eigenvalues are removed from the 'information' matrix X^TX in equation (2) so that the combinations of parameters which cannot be identified uniquely are effectively fixed. An alternative approach which has many attractive features is provided by the use of 'singular value decomposition'[17] of the matrix X.

4.1 Singular-value Decomposition

The singular value decomposition of the independent variable matrix X of equation (1) involves representing the data history by means of a new set of orthogonal variables. Solutions based upon a subset of these orthogonal variables can be shown to be equivalent to rank deficient solutions in which the most insignificant eigenvalues of the information matrix are removed.

If the matrix X involves n independent variables each having m values then it is possible to find an orthogonal nxn matrix, V, which transforms the matrix X into another mxn matrix B whose columns are orthogonal.

$$\text{i.e.} \qquad B = X\,V = (b_1\; b_2\; .\;.\;.\;.\; b_n) \qquad (18)$$

$$\text{where} \qquad b_i^T b_j = 0 \quad \text{if } i \neq j$$
$$= s_i^2 \quad \text{if } i = j \qquad (19)$$

Here the terms involving s_i^2 represent the squared magnitudes of the mx1 column vectors. The positive square roots of these terms are referred to as singular values of the matrix X. For non-zero singular values we may obtain unit orthogonal vectors u_i where

$$u_i = b_i/s_i \qquad s_i \neq 0 \qquad (20)$$

$$\text{Hence} \qquad B = U\,S \qquad (21)$$

where S is an nxn diagonal matrix with non-negative diagonal elements formed of the singular values and U is an mxn matrix whose columns are the unit orthogonal vectors u_i.

The orthogonalising matrix V upon which this approach depends may be obtained by plane rotations[17]. From equations (18) and (21) it follows that

$$X\,V = U\,S \qquad (22)$$

and therefore, because of orthogonality of V, it follows that

$$X = U\,S\,V^T \qquad (23)$$

The matrix B contains the principal components of the matrix X with each column of B representing a data history in terms of the new set of independent orthogonal variables constructed as linear combinations of the original variables.

If the mxn matrix U S is rewritten as the product of an mxm orthogonal matrix Ω, and an mxn matrix Γ having the singular values arranged in descending order of magnitude down the leading diagonal with zero elements elsewhere, equation (23) may be rewritten as

$$X = \Omega\,\Gamma\,V^T \qquad (24)$$

The least-squares solution is then obtained as

$$\Gamma^+\hat{\underline{\alpha}} = \Omega^T\underline{y} \qquad (25)$$

$$\hat{\underline{a}} = V^T\hat{\underline{\alpha}} \qquad (26)$$

where the matrix Γ^+ has elements which are the same as those of Γ but with those singular values which are smaller than a given threshold level eliminated. This allows parameter estimates to be obtained which correspond only to a subset of the dominant principal components.

From equations (1), (23) and (26) it follows that

$$\underline{y} = U\,S\,\underline{a} + \underline{\varepsilon} \qquad (27)$$

Assuming that $\underline{y}$ is not highly correlated with an orthogonal state y_{1k} associated with a small singular value (i.e. the problem is not ill-conditioned) a solution can be computed based on large singular values only. The relatively simple form of solution inherent in equations (25) and (26) also facilitates investigation of solutions using a number of different sets of singular values. It can be shown easily that the singular values of the matrix $\underline{X}$ are related to the eigenvalues of the information matrix $\underline{X}^T\underline{X}$ ($s_i = \sqrt{\lambda_i}$ where s_i is a singular value and λ_i is an eigenvalue of the information matrix). The acceptance of solutions corresponding to only a subset of the dominant principal components corresponds to the removal of the most insignificant eigenvalues of the information matrix.

The accuracy of estimates obtained by singular-value decomposition can be assessed without difficulty. It may be shown that

$$\mathrm{cov}(\hat{\underline{\alpha}} - \underline{\alpha}) = \sigma^2\, S^{-2} \tag{28}$$

and

$$\mathrm{cov}(\hat{\underline{\theta}} - \underline{\theta}) = \underline{V}\, \mathrm{cov}(\hat{\underline{\alpha}} - \underline{\alpha})\, \underline{V}^T \tag{29}$$

Here the residual variance, σ^2, may be estimated from the fit obtained using the orthogonal variables. Similarly the multiple correlation coefficient, which is a direct measure of the accuracy of fit is given by

$$R^2 = \frac{(\underline{X}\,\hat{\underline{\theta}})^T\,(\underline{X}\,\hat{\underline{\theta}})}{\underline{y}^T\,\underline{y}} \tag{30}$$

The total F-ratio provides a measure of the the confidence which can be ascribed to the fit and is defined by the equation

$$F_{TOTAL} = \frac{R^2/(p-1)}{(1 - R^2)/(m-p)} \tag{31}$$

where p is the number of parameters in the fit and m is the number of frequency values used. The partial F-ratios for individual parameters, given by

$$F_i = \hat{\theta}_i^2 \,/\, \mathrm{var}(\hat{\theta}_i - \theta_i) \tag{32}$$

provide individual parameter confidence measures.

The singular-value decomposition approach, involving only a subset of dominant principal components, thus provides a computationally convenient form of solution. The equations given above show that statistical measures of the accuracy of estimates obtained using this approach may also be determined without difficulty.

4.1.1 Application to the Pitching Moment Equation

In considering applications of the singular value decomposition method in the frequency-domain a number of important factors have to be taken into account. Firstly, it is essential to ensure that the data records are of a duration which allows parameter estimates to converge. The choice of cut-off frequency for the truncated frequency-domain record is also of great importance for accurate estimation of the parameters of rigid-body models and conventional statistical measures, such as the squared correlation coefficent and partial F-ratios, can provide useful guidance in this respect. It is essential also to establish the optimum number of orthogonal components in the singular-value decomposition and these statistical measures again can provide valuable insight. Deterministic measures of parameter significance also have a useful role in assisting in the interpretation of results of the parameter estimation process.

The pitching moment equation, for which parameter estimates were sought, may be written in normalised form in the frequency-domain as

$$\dot{Q}(\omega) = M_u\, U(\omega) + M_w\, W(\omega) + M_q\, Q(\omega) + M_v\, V(\omega) + M_p\, P(\omega) + M_{\eta_{1s}}\, \eta_{1s}(\omega) \tag{33}$$

where

$$\dot{Q}(\omega) = j\omega\, Q(\omega) + \frac{\sqrt{N}}{T}\,[q(T - \tfrac{\Delta t}{2}) - q(-\tfrac{\Delta t}{2})]\exp(j\omega\tfrac{\Delta t}{2}) \tag{34}$$

The data set used for identification in this case involved the response shown in Fig. 1 for the longitudinal cyclic doublet test input. Data from a single manoeuvre with a time-domain record of 14 seconds duration were transformed into the frequency-domain for the range 0 to 0.56 Hz., for a frequency interval of 0.07 Hz., to give eight pairs of real and imaginary values, with the values at zero frequency excluded.

Table 1 shows the parameter estimates and the associated statistical performance measures for six cases involving different numbers of orthogonal components. It may be seen from these results that the squared correlation coefficient (R^2) increases as more orthogonal components are included until with five orthogonal components any further improvement in R^2 is found to be negligible. The sixth component may well be associated mostly with noise. The standard deviation of the estimates reach their minima for the solution found with five principal components. The large

NO. OF ORTHOGONAL COMPONENTS	M_u		M_w		M_q		M_v		M_r		$M_{\eta_{1s}}$		R^2	F_{TOTAL}
	ESTIMATE	1σ ERROR BOUND	ESTIMATE	1σ ERROR BOUND	ESTIMATE	1σ ERROR BOUND	ESTIMATE	1σ ERROR BOUND	ESTIMATE	1σ ERROR BOUND	ESTIMATE	1σ ERROR BOUND		
1	-0.0009		-0.0011		0.0000		0.0001		0.0000		0.0000		0.032	0.07
2	0.0036		-0.0049		0.0000		0.0000		0.0000		-0.0006		0.408	1.37
3	0.0037		-0.0047		0.0000		0.0032		0.0000		-0.0014		0.413	1.41
4	0.0020	0.0009	-0.0024	0.0023	0.0004	0.24	-0.0032	0.0033	0.0000	0.24	-0.0286	0.0048	0.910	20.20
5 †	0.0028	0.0006	-0.0024	0.0014	-0.314	0.152	-0.0050	0.0021	-0.320	0.150	-0.0322	0.0031	0.965	54.76
6	0.0027	0.0006	-0.0037	0.0014	-0.186	0.153	-0.0059	0.0021	-0.446	0.151	-0.0304	0.0031	0.968	60.97
HELISTAB VALUES	0.0024		-0.0052		-0.835		-0.0013		-0.210		-0.0376			

†Selected model.

Table 1 Singular value decomposition solution for the pitching moment equation.
Puma, 100 Knots, longitudinal cyclic doublet input.

NO. OF ORTHOGONAL COMPONENTS	Z_w		R^2	F_{TOTAL}
	ESTIMATE	1σ ERROR BOUND		
1	-0.450	0.58	0.764	4.85
2	-0.730	0.22	0.962	37.95
3	-0.743	0.21	0.970	48.00
4	-0.781	0.14	0.988	118.90
5 †	-0.882	0.096	0.996	339.28
6	-0.918	0.098	0.996	339.28
7	-0.956	0.102	0.996	346.00
HELISTAB VALUE	-0.696			

† Selected model

Table 2 Singular value decomposition solution for the normal force solution.
Puma, 100 Knots, longitudinal cyclic doublet input.

increase in R^2 and the corresponding large reductions in the error bounds which are shown between steps 4 and 5 in Table 1 correspond to the emergence of physically more realistic estimates of parameters M_q and M_p. This improvement in the estimates of these two parameters following the introduction of the fifth orthogonal component is reflected in the matrix V by the appearance of elements of relatively large magnitude associated with M_q and M_p in the fifth row.

The effect of increasing the frequency range used for the estimation of parameters is shown in Fig. 4 in terms of the squared correlation coefficient. These results show that R^2 falls in a series of well-defined steps at frequencies of approximately 1 Hz, 5 Hz, 9 Hz and 13 Hz which correspond closely to frequencies associated with the rotor dynamics. Clearly the use of low frequency data in the estimation process eliminates these particular values and facilitates the accurate estimation of the stability and control derivatives in the six-degree-of-freedom model. Estimation of the parameters of a nine-degree-of-freedom model accounting for tip path plane dynamics as well as rigid body dynamics would, of course, require use of a wider frequency range.

Figure 5 shows the partial F-ratios for the parameters M_u, M_q and $M_{\eta 1s}$ as a function both of the frequency range used for estimation and the number of orthogonal components. The results show clearly the benefits of using five orthogonal components rather than six and also indicate that the partial F-ratios have a maximum in the low frequencies, thus confirming the significance of the low frequency range.

A large spread in the singular values can also provide an indication that some of the orthogonal components are of little importance and may be discarded as random noise. This may usually be confirmed by examination of the transformed parameter estimates corresponding to the orthogonal set and their standard deviations. In this application all the evidence suggested that the parameter estimates for M_p and M_q for six orthogonal components were greatly in error in comparison with those for five components and should therefore be discarded.

A number of measures of the significance of individual parameters have been proposed for identification in the time-domain. One such measure is based upon the integral of the absolute value of the variable associated with the chosen parameter multiplied by the estimate obtained for that parameter and divided by the integral of the absolute value of the dependent variable of the equation[18]. In the case of the pitching moment equation in the time-domain this leads to measures such as

$$|M_u| \int |u| dt \;/\; \int |\dot{q}| dt$$

and

$$|M_w| \int |w| dt \;/\; \int |\dot{q}| dt$$

Corresponding measures may be derived in the case of frequency-domain identification with the integration being carried out over the range of frequency values selected and the magnitude of the Fourier transformed quantities being used in place of the magnitude of the time-domain responses. These frequency-domain measures of parameter significance therefore take the form

$$|M_u| \int |U(\omega)| d\omega \;/\; \int |\dot{Q}(\omega)| d\omega$$

and

$$|M_w| \int |V(\omega)| d\omega \;/\; \int |\dot{Q}(\omega)| d\omega$$

Figure 6 shows parameter significance values for each set of principal components for frequency-domain data using the range 0 – 0.56 Hz. These results show the importance of M_u, M_w and $M_{\eta 1s}$ in the first few principal component solutions. However, the solution obtained using the first five principal components, and accepted as the best least-squares solution, shows significance values of similar magnitude for M_u, M_w, M_q and M_p. It should be pointed out that the solution corresponding to six orthogonal components is the one that would be obtained using the conventional least-squares approach involving the direct application of equation (2).

Figure 7 shows the effect of the record length on parameter estimates for the frequency range used above. The estimates are seen to reach almost constant values as the record length approaches the 14 seconds duration which was used for all of the results given above. The standard errors clearly tend to lower values as the record length is increased. All of these findings support the choice of record length adopted and show very clearly the problems of accurate estimation from shorter records. Long records are also desirable in frequency-domain estimation from the point of view of resolution. It is of interest to note that the parameters in Table 1 estimated with greatest confidence (M_u, $M_{\eta 1s}$) approach their final estimated values for much shorter record lengths than some of the other parameters such as M_q, M_v and M_p and that these latter parameter estimates have larger standard deviations.

Since actual experimental flight data have been analysed in this application there is no set of 'true parameters' to which estimates can be compared. The helicopter flight mechanics package HELISTAB[19,20] provides theoretical parameter values which may be considered alongside the estimates obtained from flight data. HELISTAB predictions for the parameters of the pitching moment equation are included in Table 1 and it may be seen that the most significant discrepancy is in the parameter M_q.

NO. OF ORTHOGONAL COMPONENTS	M_u		M_w		M_q		M_v		M_p		$M_{\eta 0}$		$M_{\eta 1s}$		$M_{\eta 1c}$		R^2	F_{TOTAL}
	ESTIMATE	1σ ERROR BOUND	ESTIMATE	1σ ERROR BOUND	ESTIMATE	1σ ERROR BOUND	ESTIMATE	1σ ERROR BOUND	ESTIMATE	1σ ERROR BOUND	ESTIMATE	1σ ERROR BOUND	ESTIMATE	1σ ERROR BOUND	ESTIMATE	1σ ERROR BOUND		
6	0.0014	0.0003	-0.0041	0.0010	0.0005	0.165	-0.0026	0.0008	0.0002	0.076	0.0075	0.0024	-0.0302	0.0041	0.0036	0.0028	0.771	29.78
7 †	0.0015	0.0003	-0.0040	0.0009	-0.0593	0.150	-0.0046	0.0007	-0.1965	0.0696	0.0071	0.0022	-0.0325	0.0037	-0.0002	0.0025	0.809	37.42
8	0.0015	0.0003	-0.0036	0.0009	-0.1370	0.151	-0.0046	0.0007	-0.1728	0.070	0.0077	0.0022	-0.0335	0.0037	0.0004	0.0025	0.810	37.73
HELISTAB VALUES	0.0024		-0.0051		-0.835		-0.0013		-0.210				-0.0376					

†Selected model.

Table 3a Singular value decomposition solution for the pitching moment equation.
Puma, 100 Knots, multirun case, all four controls used.

NO. OF ORTHOGONAL COMPONENTS	Z_w		$Z_{\eta 0}$		R^2	F_{TOTAL}
	ESTIMATE	1σ ERROR BOUND	ESTIMATE	1σ ERROR BOUND		
8	-0.7950	0.120	-0.632	0.253	0.816	33.69
9 †	-0.7093	0.119	-0.689	0.251	0.820	34.77
HELISTAB VALUE	-0.696		-0.732			

† Selected model

Table 3b Singular value decomposition solution for the normal.
force equation.
Puma, 100 Knots, multirun case, all four controls used.

4.1.2 Application to the Normal Force Equation

The singular value decomposition approach has been applied to the estimation of parameters of the normal force equation

$$(\dot{W}(\omega) - U_e\ Q(\omega)) = Z_u\ U(\omega) + Z_w\ W(\omega) + Z_\theta\ \theta(\omega) + Z_v\ V(\omega) + Z_p\ P(\omega) + Z_q\ Q(\omega) + Z_\phi\ \phi(\omega) + Z_{\eta_{1s}}\ \eta_{1s}(\omega) \qquad (35)$$

Values for $\dot{W}(\omega)$ over the frequency range of interest can be obtained from equations (15) and (16). The quantity U_e represents the forward trim velocity and the term $U_e\ Q(\omega)$ arises in the linearisation of the equations of motion.

Results obtained from the test data relating to the response to a longitudinal cyclic doublet are given in Table 2. The data again relate to the response of the Puma to a longitudinal cyclic doublet for a forward trim speed of approximately 100 knots with a record length of 14 seconds. The upper limit of the frequency range was 0.56 Hz. with zero frequency excluded and with eight values of frequency used at an interval of 0.07 Hz.. The results indicate that the only significant parameter on the right hand side of equation (35) is Z_w and examination of R^2 and the standard deviations of the estimated orthogonal parameters suggests that the use of only the first five orthogonal components produces the best results since parameters associated with the other singular values are estimated with a high degree of uncertainty. The slightly higher R^2 values for the fits which are obtained by including the sixth and seventh orthogonal components involve parameters estimated with a high degree of uncertainty and are therefore discounted. It is believed that the simpler model based upon the first five orthogonal components is to be preferred. Figure 8 shows parameter significance data for the parameters of the normal force equation and illustrates very clearly the dominance of the parameter Z_w.

4.1.3 Parameter Estimation from Multirun Data

When only one control input is used to excite all of the rigid body modes poor estimates are often obtained for the parameters associated with states which play an insignificant part in the resulting aircraft motion. Such parameters show low values in terms of the parameter significance measures (typically less than 0.1) and low partial F values.

Since it is impractical to apply more than one test input at a time on more than one control by manual methods, it has been recognised that data from a number of different manoeuvres must often be used for identification purposes. One approach involves stacking the data to produce a single long run from a series of shorter runs for different test inputs[18]. Since regression is based upon the correlation between variables the discontinuities at manoeuvre boundaries do not affect the results.

Results are presented in Table 3 for a combination of four manoeuvres, as shown in Fig. 9. The inputs involved all four controls and consisted of a collective doublet, a longitudinal cyclic 3211 input, a pedal doublet and a lateral cyclic step input. Compared with the previous single manoeuvre case for the pitching moment equation, the estimated standard errors are smaller for the pitching moment cross-coupling terms M_v and M_p. The M_p estimate compares well with the theoretical HELISTAB value. The M_v estimate, although different from the theoretical prediction, is consistent with the value found in the previous case of the longitudinal cyclic doublet input. The $M_{\eta_{1s}}$ estimates show a similar consistency for the two cases. The M_w value now obtained is much closer to theory than the value found from the single input case, although the estimated value of M_q is significantly different. For the normal force equation the Z_w estimate compares very well with theory.

Solutions were obtained using seven orthogonal components for the pitching moment equation, nine components for the normal force equation, and ten components each for the rolling moment and yawing moment equations. The numbers of independent (non-orthogonal) variables included in the original model in each of the above cases were eight, nine, ten and ten respectively. The standard errors of the estimates reached their minima for the chosen components.

The frequency range used extends to 0.5 Hz. with the estimation carried out at thirty five different frequencies. It should be noted that, although some of the standard errors are reduced in comparison with the case for the single manoeuvre, the squared correlation coefficient value was also reduced. The benefits of multirun estimation may have been reduced in this case by the fact that the lateral cyclic input involved a step rather than an input having a zero mean, such as a doublet or 3211. This choice of lateral input was dictated by the available test records for the chosen flight condition of nominally 100 knots.

Transformation of the state equation

$$\dot{\mathbf{x}}(t) = A\,\mathbf{x}(t) + B\,\mathbf{u}(t) \tag{36}$$

into the frequency-domain using the discrete Fourier transform yields, as already shown, an equation of the form

$$j\omega\,\mathbf{X}(\omega) = A\,\mathbf{X}(\omega) + B\,\mathbf{U}(\omega) - \frac{\sqrt{N}}{T}\left[\mathbf{x}\left(T - \frac{\Delta t}{2}\right) - \mathbf{x}\left(-\frac{\Delta t}{2}\right)\right]\exp\left(\frac{j\omega\Delta t}{2}\right) \tag{37}$$

Equation (37) may be rewritten in the form

$$\begin{bmatrix} -A & . & -\omega I \\ \cdots & \cdots & \cdots \\ \omega I & . & -A \end{bmatrix}\begin{bmatrix} \mathrm{Re}[\mathbf{X}(\omega)] \\ \cdots \\ \mathrm{Im}[\mathbf{X}(\omega)] \end{bmatrix} = \begin{bmatrix} B & . & 0 \\ \cdots & \cdots & \cdots \\ 0 & . & B \end{bmatrix}\begin{bmatrix} \mathrm{Re}[\mathbf{U}(\omega)] \\ \cdots \\ \mathrm{Im}[\mathbf{U}(\omega)] \end{bmatrix} - \frac{\sqrt{N}}{T}\begin{bmatrix} \Delta\mathbf{x}\cos\frac{\omega\Delta t}{2} \\ \cdots \\ \Delta\mathbf{x}\sin\frac{\omega\Delta t}{2} \end{bmatrix} \tag{38}$$

where Re and Im indicate real and imaginary parts respectively, I is the identity matrix, O is the null matrix and $\Delta\mathbf{x} = \mathbf{x}(T-\frac{\Delta t}{2}) - \mathbf{x}(-\frac{\Delta t}{2})$

In general, in the time-domain, the states $\mathbf{x}(t)$ are related to the measured quantities, $\mathbf{z}(t)$, by an equation of the form

$$\mathbf{z}(t) = H\,\mathbf{x}(t) + \mathbf{k} + \mathbf{b} \tag{39}$$

If the full model output vector is defined in the frequency-domain as

$$\underline{X}(\omega) = L\,\mathbf{X}(\omega) \qquad \omega \neq 0 \tag{40}$$

where

$$L = \begin{bmatrix} H & . & 0 \\ \cdots & \cdots & \cdots \\ 0 & . & H \end{bmatrix}$$

then a suitable choice of cost function has the form

$$J = \sum_{\omega_1}^{\omega_2} [\check{\underline{Z}}(\omega) - \check{\underline{X}}(\omega)]^T\,\bar{W}[\check{\underline{Z}}(\omega) - \check{\underline{X}}(\omega)] + \log_e|W^{-1}| \tag{41}$$

where

$$\check{\underline{X}}(\omega) = \begin{bmatrix} \mathrm{Re}[\underline{X}(\omega)] \\ \cdots \\ \mathrm{Im}[\underline{X}(\omega)] \end{bmatrix} \qquad \check{\underline{Z}}(\omega) = \begin{bmatrix} \mathrm{Re}[\underline{Z}(\omega)] \\ \cdots \\ \mathrm{Im}[\underline{Z}(\omega)] \end{bmatrix}$$

$$\check{\mathbf{U}}(\omega) = \begin{bmatrix} \mathrm{Re}[\mathbf{U}(\omega)] \\ \cdots \\ \mathrm{Im}[\mathbf{U}(\omega)] \end{bmatrix} \qquad \text{and} \qquad \bar{W} = \begin{bmatrix} W & . & 0 \\ \cdots & \cdots & \cdots \\ 0 & . & W \end{bmatrix}$$

W is a real valued diagonal weighting matrix and although this matrix can involve elements which remain fixed in value throughout, the current implementation is based upon the use of fixed elements for the first few iterations with subsequent estimation of the elements of W from the expected and actual outputs. The values used for the initial phase, where the elements of W are fixed, reflect the initial estimates of the relative noise levels on the measurements.

The frequency-domain approach facilitates the incorporation of time-delays within the model[21]. These time delays may be present in both the measured responses and in the control inputs. In the latter case the control term in equation (38) must be modified to give[22], for the case of r controls

$$\begin{bmatrix} B & . & 0 \\ \cdots & \cdots & \cdots \\ 0 & . & B \end{bmatrix}\left[\begin{array}{cccc:cccc} \cos\omega\tau_1 & & & 0 & \sin\omega\tau_1 & & & 0 \\ & \cos\omega\tau_2 & & & & \sin\omega\tau_2 & & \\ & & \ddots & & & & \ddots & \\ 0 & & & \cos\omega\tau_r & 0 & & & \sin\omega\tau_r \\ \hdashline -\sin\omega\tau_1 & & & 0 & \cos\omega\tau_1 & & & 0 \\ & -\sin\omega\tau_2 & & & & \cos\omega\tau_2 & & \\ & & \ddots & & & & \ddots & \\ 0 & & & -\sin\omega\tau_r & 0 & & & \cos\omega\tau_r \end{array}\right]\check{\mathbf{U}}(\omega)$$

The r delay parameters $\tau_1, \tau_2, \ldots \tau_r$, each associated with a control $U_1(\omega)$, $U_2(\omega), \ldots\ldots U_r(\omega)$, can then be included in the set of parameters for which estimates are sought. Such time delay elements may result from a number of factors including a time lag between initiation of a control signal and the response of the actuators, phase shifts due to filtering of the data, or unmodelled features of the real system (e.g. rotor dynamics).

In general J is a function of the system matrix A, the control input matrix B, the measurement transition matrix H, the time delays and the frequency range $(\omega_2-\omega_1)$ used for the estimation. Minimisation of this cost function with respect to a vector $\underline{\theta}$ of m unknown parameters requires that the condition

$$\left[\frac{\partial}{\partial\theta_1} \quad \frac{\partial}{\partial\theta_2} \quad \cdots\cdots\cdots \quad \frac{\partial}{\partial\theta_m}\right]^T J \quad = \underline{0} \tag{42}$$

be satisfied.

Using a line search modification[23] to the basic Newton-Raphson method, an optimisation technique has been developed from which parameter estimates are obtained in a computationally efficient manner over the selected frequency range. The transformation of the problem into the frequency-domain means that algebraic expressions can be found for each stage of the minimisation process where equivalent steps in the time-domain implementation require numerical integration. In addition, the parameter covariance matrix can be determined for the chosen frequency range using an approach analogous to that applied in the time-domain[24], the actual bandwidth of the measurement being an important factor to be taken into account in modelling the error[25].

5.1 Application of the Output-Error Approach to Identification of Longitudinal Dynamics

The mathematical model given below in equation (43) has provided a basis for estimation of the longitudinal parameters of the six-degree-of-freedom rigid-body model. In this equation all of the significant longitudinal/lateral coupling terms (as determined from parameter significance measures of the type already defined) are incorporated in an extended control vector.

$$\begin{bmatrix} \dot{u}(t) \\ \dot{w}(t) \\ \dot{q}(t) \\ \dot{\theta}(t) \end{bmatrix} = \begin{bmatrix} X_u & X_w & X_q - V_e & X_\theta - g\cos\theta_e \\ Z_u & Z_w & Z_q + U_e & Z_\theta - g\sin\theta_e \\ M_u & M_w & M_q & 0 \\ 0 & 0 & 1 & 0 \end{bmatrix} \begin{bmatrix} u(t) \\ w(t) \\ q(t) \\ \theta(t) \end{bmatrix}$$

$$+ \begin{bmatrix} 0 & 0 & X_{\eta_{1s}} \\ 0 & Z_p & Z_{\eta_{1s}} \\ M_\beta & M_p & M_{\eta_{1s}} \\ 0 & 0 & 0 \end{bmatrix} \begin{bmatrix} \beta(t) \\ p(t) \\ \eta_{1s}(t-\tau) \end{bmatrix} \tag{43}$$

The measured variables are related to the state variables by the additional equation

$$\begin{bmatrix} V(t) \\ \alpha(t) \\ q(t) \\ \theta(t) \end{bmatrix} = \begin{bmatrix} S_v & 0 & l_x^{v} & 0 \\ 0 & S\alpha/U_e & -l_x^{\alpha}/U_e & 0 \\ 0 & 0 & 1 & 0 \\ 0 & 0 & 0 & 1 \end{bmatrix} \begin{bmatrix} u(t) \\ w(t) \\ q(t) \\ \theta(t) \end{bmatrix}$$

$$+ \begin{bmatrix} V_{bias} \\ \alpha_{bias} \\ q_{bias} \\ \theta_{bias} \end{bmatrix} \tag{44}$$

A number of the coefficients in these equations are known to be very small for the conditions used in the test and, on the basis of their parameter significance values, several have been excluded from the estimation process. Initial parameter estimates for the output-error method must be provided from results obtained using the equation-error approach, or from theoretical model values, to ensure rapid convergence of the output-error algorithm.

Application of the output-error method to the flight data used in the equation-error applications of Sections 4.1.1 and 4.1.2 for the longitudinal cyclic doublet input provided the results shown in Table 4. The frequency range used involved the eight spectral lines up to 0.56 Hz, as before, with zero frequency again excluded. In this implementation of the output-error approach the diagonal weighting matrix elements were assigned initial values based upon estimated noise variances. This allowed some initial convergence of the estimation process to take place before the introduction of the updating of the weighting matrix elements at each subsequent iteration using actual and estimated model outputs.

PARAMETER	ESTIMATE	1 σ ERROR BOUND	HELISTAB VALUE
M_u	0.00319	0.00021	0.0024
M_w	-0.00252	0.00070	-0.0051
M_q	-0.353	0.091	-0.835
M_θ †	-1.225	0.090	
M_p	-0.412	0.069	-0.210
$M_{\eta_{1s}}$	-0.0308	0.0017	-0.0376
Z_u	0.0504	0.022	-0.0316
Z_w	-0.805	0.021	-0.696
$Z_{\eta_{1s}}$	0.699	0.14	0.618
X_u	-0.0384	0.037	-0.0265
$X_{\eta_{1s}}$	0.599	0.33	0.180

†M_v = -0.00764

Table 4 Parameter estimates obtained by output-error method.

Figure 10 shows comparisons of the actual and estimated power spectra with the number of iterations in the estimation process. The model results and the flight data match very closely in the frequency-domain after three iterations. Although Fig. 10 only shows the results for the case where incidence angle is the variable considered, similar results have been found for the pitch rate and pitch attitude variables. In the case of the forward speed the match between the measured and estimated spectra was less satisfactory, especially in the middle of the frequency range considered, but it must be recognised that this measured quantity shows relatively little power at the mid-range and upper frequencies in comparison with the other measurements.

Results have also been obtained for the case where a time delay is postulated in the longitudinal cyclic input and these are shown in Table 5. Most of the pitching moment terms, even those estimated with small error bounds, show some change in the estimated values when this time delay parameter is introduced and for parameters M_p and M_q these changes are significant. These alterations in the identified pitching moment derivatives may be due partly to effects associated with rotor dynamics being lumped into the fuselage coefficients in the case where no time delay is incorporated in the model.

PARAMETER	ESTIMATE	1 σ ERROR BOUND	HELISTAB VALUE
M_u	0.00419	0.00040	0.0024
M_w	-0.00022	0.0012	-0.0051
M_q	-0.823	0.18	-0.835
M_θ †	-1.306	0.10	
M_p	-0.248	0.086	-0.210
$M_{\eta_{1s}}$	-0.0396	0.0034	-0.0376
Z_u	0.0362	0.021	-0.0316
Z_w	-0.796	0.019	-0.696
$Z_{\eta_{1s}}$	0.520	0.12	0.618
X_u	-0.0319	0.033	-0.0265
$X_{\eta_{1s}}$	0.969	0.34	0.180
τ	0.134	0.037	

† M_v = -0.0081

Table 5 Parameter estimates obtained by output-error method. Time delay parameter included in longitudinal cyclic input.

6. TRANSFER FUNCTION ESTIMATION IN THE FREQUENCY-DOMAIN

The use of single-input, single-output transfer functions valid over a defined frequency range for chosen flight conditions provides an approach which has been found, by Tischler et al.[12], to give good results. The classical pitch rate and normal acceleration responses to a longitudinal cyclic input for the short period mode are given by the following equations

$$\frac{Q(s)}{\eta_{1s}(s)} = \frac{M_{\eta_{1s}}\ (s + 1/T_\theta)\ \exp(-s\tau_\theta)}{s^2 + 2\zeta\omega_{sp} + \omega_{sp}^2} \tag{45}$$

$$\frac{A_z(s)}{\eta_{1s}(s)} = \frac{Z_{\eta_{1s}}\ \exp(-s\tau_{az})}{s^2 + 2\zeta\omega_{sp} + \omega_{sp}^2} \tag{46}$$

In equation (45) the term $Q(s)/\eta_{1s}(s)$ is the Laplace-transformed pitch rate response to a longitudinal cyclic input. The parameter $M_{\eta_{1s}}$ is the longitudinal cyclic pitch sensitivity and τ_θ is the effective time delay on the input for pitch rate. The parameter T_θ is given by[26]

$$T_\theta = \frac{M_{\eta_{1s}}}{M_w\ Z_{\eta_{1s}} - Z_w\ M_{\eta_{1s}}} \tag{47}$$

while ζ and ω_{sp} are the equivalent short-period mode damping and natural frequency respectively. In equation (46) the term $A_z(s)/\eta_{1s}$ is the Laplace-transformed normal acceleration response to a longitudinal cyclic input, while $Z_{\eta_{1s}}$ is the longitudinal cyclic normal force sensitivity. The effective time delay on the input, τ_{az}, was for this case, assumed negligible. The denominator parameters are identical to those in the pitch rate transfer function.

Equations (45) and (46) may be written in state space form in the time-domain as

$$\begin{bmatrix} \dot{q}(t) \\ \ddot{q}(t) \\ \dot{a}_z(t) \\ \ddot{a}_z(t) \end{bmatrix} = \begin{bmatrix} 0 & 1 & 0 & 0 \\ -\omega_{sp}^2 & -2\zeta\omega_{sp} & 0 & 0 \\ 0 & 0 & 0 & 1 \\ 0 & 0 & -\omega_{sp}^2 & -2\zeta\omega_{sp} \end{bmatrix} \begin{bmatrix} q(t) \\ \dot{q}(t) \\ a_z(t) \\ \dot{a}_z(t) \end{bmatrix}$$

$$+ \begin{bmatrix} 0 & 0 & 0 \\ M_{\eta_{1s}}/T_\theta & M_{\eta_{1s}} & 0 \\ 0 & 0 & 0 \\ 0 & 0 & Z_{\eta_{1s}} \end{bmatrix} \begin{bmatrix} \eta_{1s}(t - \tau_\theta) \\ \dot{\eta}_{1s}(t - \tau_\theta) \\ \eta_{1s}(t - \tau_{az}) \end{bmatrix} \tag{48}$$

The estimation problem is now formulated in a way that allows use to be made of the frequency-domain output-error approach outlined in the previous sections. The ease with which parameters within this model structure can be related when the output-error method is used is a significant advantage in this case since the parameters $-\omega_{sp}^2$, $2\zeta\omega_{sp}$ and τ_θ all occur twice. By specifying the equalities existing among the elements in the second and fourth rows of the state matrix of equation (48) we are effectively imposing equality in the denominator coefficients for the transfer functions shown in equations (45) and (46).

Using the measured response data from the flight test involving the application of a longitudinal cyclic test input, estimates were obtained by the method outlined above for ω_{sp}^2, $2\zeta\omega_{sp}$ etc. The complete set of parameter values, together with their error bounds and theoretical predictions obtained from HELISTAB, are presented in Table 6.

If a value of -0.8 is assumed for the parameter Z_w, which is consistent with the estimates Tables 2,3,4 and 5, the relationships

$$Z_w + M_q = -2\zeta\omega_{sp} \tag{49}$$

and

$$Z_w\ M_q - M_w\ U_e \approx \omega_{sp}^2 \tag{50}$$

may be used to give estimates of M_q and M_w of -0.85 and -0.0012 respectively. It is of interest to compare these values with the corresponding figures in Tables 4 and 5 and to note the close agreement with the HELISTAB prediction in the case of M_q.

PARAMETER	ESTIMATE	1 σ ERROR BOUND	HELISTAB VALUE
ω_{sp}^2	0.877	0.45	0.93
$2\zeta\omega_{sp}$	1.655	0.29	1.76
$M_{\eta 1s}/T_\theta$	−0.0269	0.014	
$M_{\eta 1s}$	−0.0407	0.007	−0.0376
$Z_{\eta 1s}$	3.69	1.63	0.618
τ_θ	0.195	0.08	

Table 6 Single input - single output transfer function values.

7 DISCUSSION

Although the results shown in Tables 1, 2 and 3 for the equation-error method provide an indication of the quality of parameter estimates in terms of the standard deviation of the estimates themselves, the squared correlation coefficient and F-ratio values, further evidence of the overall validity of an identified model can be obtained by comparing measured response spectra with the corresponding predicted spectra. Figure 11 shows frequency-domain comparisons of this type for the pitching moment and normal force equations for the longitudinal cyclic doublet input. In the case of the pitching moment equation the plots show the fit obtained using the parameter sets estimated with four, five and six orthogonal components. For five orthogonal components the fit obtained is good over the whole of the frequency range considered and this provides useful confirmation of the model selected earlier. The corresponding curves for the normal force equation are shown for up to six orthogonal components. Taken in conjunction with the statistical measures shown in Table 2 the results again support the earlier choice of a model based upon five orthogonal components.

Figure 12 shows actual and predicted frequency-domain results for the variables p, q and r, together with the normal force for the multirun case. This comparison is presented for the identification based upon the optimum set of orthogonal components as given in Section 4.1.3. The number of frequencies at which comparisons can be made is, of course, much greater than in the previous two cases and the overall agreement is excellent.

Reconstructions in the time-domain (obtained by integrating the identified state space model at each time step) can also provide a useful basis for the verification of a model involving parameters estimated using a frequency-domain approach. Figure 13 gives an interesting illustration of this time-domain verification process, where the pitch rate response is shown for the parameter sets obtained using the output-error approach both with and without a time delay. The agreement between the measured and model outputs is seen to be especially close for the model that was identified with a time delay element included in the control input. The match is particularly good during the first six seconds of the record. In both cases the agreement is poorer towards the end of the record. This deterioration may be due to the fact that at the end of the record several variables are at their maximum excursion from the trim level and a linear model may be least appropriate at this point.

It is also important to verify models using inputs other than those upon which the parameter estimates are based. Figure 14 provides an example of this type of assessment where spectra are shown for the response to a longitudinal cyclic DFVLR '3211', together with predictions based on the identified model using the longitudinal cyclic doublet described earlier. The response to a longitudinal cyclic doublet input, and predictions based on the multirun model described earlier are also shown. The overall agreement between the measured and predicted response is good in both cases.

Figure 15 shows comparisons of parameter estimates from Tables 1 - 6 with corresponding values predicted by the HELISTAB helicopter flight mechanics package. Error bounds associated with these parameter estimates are shown by means of dashed lines. In the pitching moment equation,for example, the four estimates obtained for the stability derivative M_u have a mean value of 0.0029 which is very close to the HELISTAB prediction of 0.0024. For the derivative M_w it may be seen that the HELISTAB prediction represents a more stable aircraft than is suggested by the parameter estimates. Some correlation is also evident between the parameter estimates obtained for M_w and those for M_q.

Estimates of the pitch damping parameter M_q differ significantly from the predicted value in all cases except that for the output-error method with the delay incorporated. The value of M_q in Table 5 and the result calculated using the transfer function approach are both very close to the theoretical value from the HELISTAB program. This is encouraging in that good estimates of this parameter are known to be difficult to obtain by conventional time-domain methods due to the contribution of rotor dynamics to the short term pitch response to sharp edged cyclic control inputs[8]. The derivative M_p is also seen to be in close agreement with the predicted value for the output-error method with the time delay parameter incorporated in the model.

One parameter which shows considerable consistency in its estimates is Z_w. This derivative, which is the only significant parameter estimated in the normal force equation also shows small values of error bound. The estimated values are close to the value predicted by HELISTAB.

It is important to note that the error bounds for estimates obtained from the equation-error method and the output-error approach are not directly commensurable since the assumtions made in modelling the error are different in the two cases. In the equation-error method it is assumed that there is no uncertainty in the independent states and biased estimates will result if there is. In the output-error method, on the other hand, unbiased estimates can in principle be obtained, to a first degree of approximation, from measurements corrupted by noise.

With reference to the multirun approach discussed in Section 4.1.3 it has been stated elsewhere that this approach does not always lead to improved estimates[5]. In some cases parameters which are estimated well in the single run case have degraded estimates when a combined or stacked data set is used for the estimation, although cross-coupling parameters may well be better estimated using multirun data. An alternative approach has been proposed, known as the method of successive residuals[5], which involves a systematic process for combining estimates from single manouevres. Encouraging results have been obtained for the estimation of cross-coupling derivatives using this approach with simulated data from linear models. No experience has so far been gained in the current programme of research in the application of this method to real flight data.

Other major continuing topics of research include consideration of the range of validity of six degree-of-freedom models across a much wider flight envelope. Estimation of model structures and parameters for rotor degrees-of-freedom is also being explored using simulation data and measurements from the RAE Puma. In a further development, control inputs aimed at minimising the number of singular values in the information matrix are being designed to increase the effectiveness of flight testing.

8 CONCLUSIONS

The results presented in this paper show that frequency-domain techniques provide a useful basis for helicopter parameter identification, both in terms of equation-error and output-error methods. The flexibility of the frequency-domain approach in allowing a restricted range of frequencies to be considered in the identification of a six-degree-of-freedom model has been shown to provide important practical benefits using real flight data. Particularly encouraging are the good results obtained in cases where estimates by conventional time-domain methods are known to be adversely affected by rotor modes not included in the rigid-body model.

Singular value decomposition has been shown to provide a useful alternative to rank deficient solutions, and examples using flight data have demonstrated the fact that improved parameter estimates may be obtained from solutions based upon appropriate subsets of the available orthogonal components. Software developed for the implementation of equation-error methods based upon the singular value decomposition approach now forms an important element of the integrated tool-kit for helicopter parameter identification which is being developed jointly by RAE (Bedford) and Glasgow University. This software for singular value decomposition allows the user to explore rapidly, and with ease, the effect of varying the number of orthogonal components and to select, on the basis of appropriate statistical measures, the optimum set of components.

An output-error method, specifically for frequency-domain estimation, has been developed. A significant feature of the method is the ease with which time delays can be incorporated within the estimation procedure. Initial results have suggested that the inclusion of these delay elements can lead to improved estimates for parameters such as M_q in the pitching moment equation.

The frequency-domain output-error method has been used successfully to estimate the damping factor, natural frequency and other parameters of single-input single-output transfer descriptions. Preliminary results obtained by this method are encouraging and have provided estimates of stability derivatives which are in close agreement with values predicted by the theoretical HELISTAB model.

The experience reported in this paper has served to increase confidence that robust and reliable methods can be established for helicopter system identification. U.K. research continues to strive to meet this objective.

9 ACKNOWLEDGEMENT

The research on helicopter parameter identification carried out at the University of Glasgow is supported by the U.K. Ministry of Defence (Procurement Executive) through Agreement No. 2048/028 XR/STR.

REFERENCES

1. Parameter Identification. AGARD LS-104, 1979.

2. R.E. Maine, K.W. Iliff — Identification of Dynamic Systems. AGARD AG-300-Vol.2, 1985.

3. J.A. Molusis — Rotorcraft Derivative Identification from Analytical Models and Flight Test Data. AGARD CP-172, 1974.

4. W.E. Hall Jr., N.K. Gupta, R.S. Hanson — Rotorcraft System Identification Techniques for Handling Qualities and Stability and Control Evaluation. 34th. AHS National Forum, Washington, May 1978.

5. R.W. DuVal, J.C. Wang, M.Y. Demiroz — A Practical Approach to Rotorcraft System Identification. 39th. AHS National Forum, St. Louis, May 1983.

6. J. Kaletka — Practical Aspects of Helicopter Parameter Identification. AIAA Atmospheric Flight Mechanics Conference, Seattle, August 1984.

7. G.D. Padfield, R.Thorne, D. Murray-Smith, C. Black A.E. Caldwell — UK Research into System Identification for Helicopter Flight Mechanics. 11th. European Rotorcraft Forum, London, September 1985, Paper 82.

8. G.D. Padfield — Integrated System Identification Methodology for Helicopter Flight Dynamics. 42nd. AHS National Forum, Washington, June 1986.

9. V. Klein — Maximum Likelihood Method for Estimating Airplane Stability and Control Parameters from Flight Data in Frequency Domain. NASA TR-1637, 1980.

10. R.W. DuVal — The Use of Frequency Methods in Rotorcraft System Identification. AIAA 1st. Flight Testing Conference, Las Vegas, November 1981 (AIAA-81-2386).

11. K.H. Fu, M. Marchand — Helicopter System Identification in the Frequency Domain. 9th. European Rotorcraft Forum, Stresa, 1983, Paper 96.

12. M.B. Tischler, L.G.M. Leung, D.C. Dugan — Frequency Domain Identification of XV-15 Tilt Rotor Aircraft Dynamics. AIAA 2nd. Flight Testing Conference, Las Vegas, November 1983 (AIAA-83-2695).

13. G.W. Foster — A Description of the Weighted Least Squares Output Error Method of Parameter Identification. RAE Technical Memorandum FS 215, 1978.

14. NAG-Fortran Library Manual, Mark 11, Vol. 1, Numerical Algorithms Group Ltd., Oxford, 1984.

15. W.E. Hall Jr., J.G. Bohn, J.H. Vincent — Development of Advanced Techniques for Rotorcraft State Estimation and Parameter Identification. NASA CR 159297, 1980.

16. D.E. Stepner, R.K. Mehra — Maximum Likelihood Identification and Optimal Input Design for Identifying Aircraft Stability and Control Derivatives. NASA CR 2200, 1973.

17. J.C. Nash — 'Compact Numerical Methods for Computers: Linear Algebra and Function Minimisation'. Hilger, Bristol, 1979.

18. J. Kaletka — Rotorcraft Identification Experience. AGARD LS-104, 1979, Paper 7.

19. J. Smith — An Analysis of Helicopter Flight Mechanics: Part 1 - Users Guide to the Software Package HELISTAB. RAE Technical Memo. FS(B) 569, 1984.

20. G.D. Padfield, J. Smith — An Analysis of Helicopter Flight Mechanics: Part 2 - Theory for the Software Package HELISTAB. RAE Technical Report (in preparation).

21. M. Marchand, K.H. Fu
Frequency Domain Parameter Estimation of Aeronautical Systems without and with Time Delay.
In H.A. Barker, P.C. Young (editors), 'Identification and System Parameter Estimation 1985', Pergamon Press, 1985, pp. 669-674.

22. C.G. Black
A Frequency-Domain Output-Error Method of Parameter Estimation: Development of Method and Computer Implementation.
University of Glasgow, Department of Aeronautics and Fluid Mechanics, Report 8603, 1986.

23. G.W. Foster
The Identification of Aircraft Stability and Control Parameters in Turbulence.
RAE Technical Report 83025, 1983.

24. V. Klein
Identification Evaluation Methods.
AGARD LS-104, 1979, Paper 2.

25. R.E. Maine, K.W. Iliff
The Theory and Practice of Estimating the Accuracy of Dynamic Flight-Determined Coefficients.
NASA Reference Publication 1077, 1981.

26. G.D. Padfield
On the Use of Approximate Models in Helicopter Flight Mechanics.
6th. European Rotorcraft and Powered Lift Aircraft Forum, Bristol, September 1980, Paper 57.

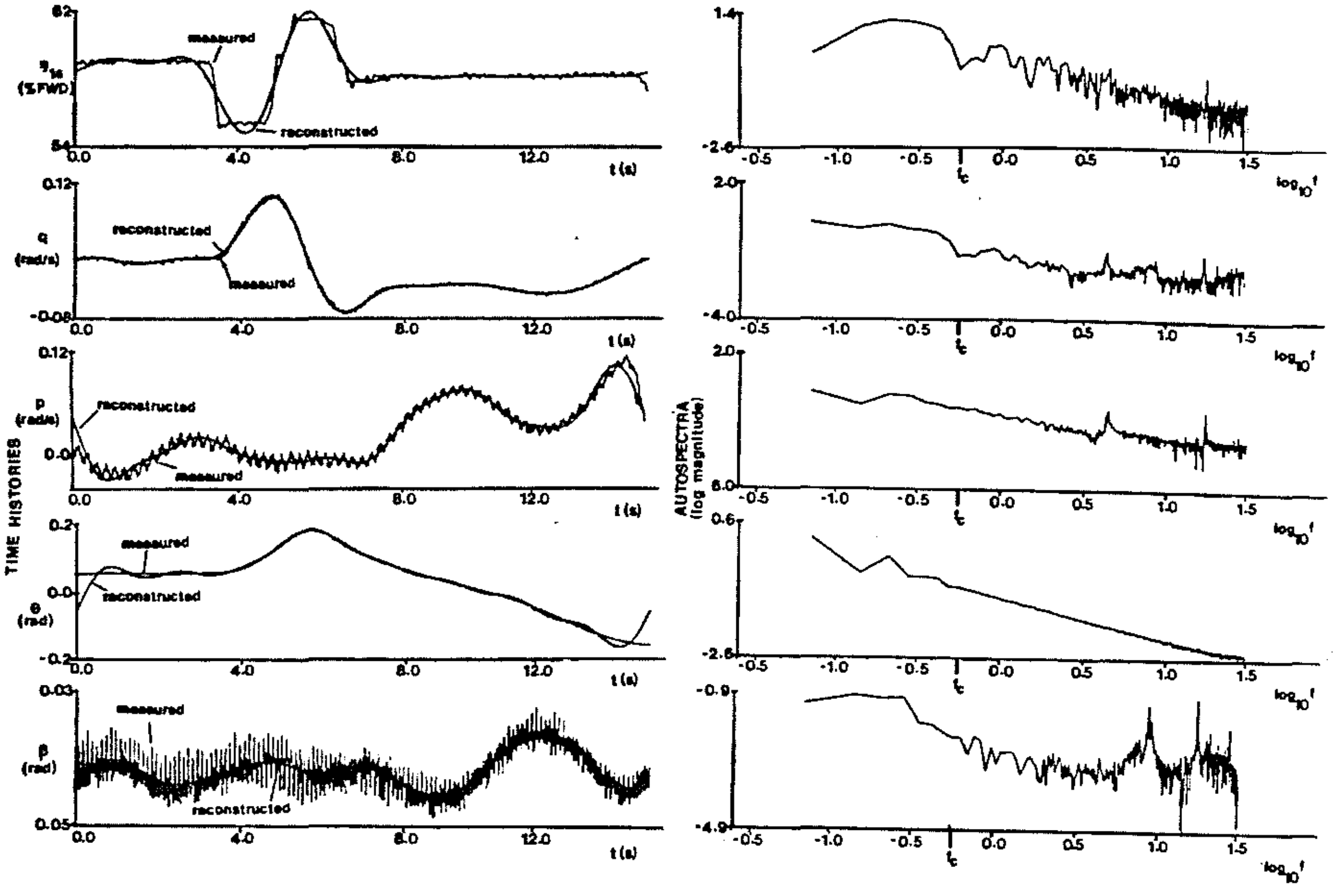

Figure 1. Measured time histories and corresponding power spectra in response to longitudinal cyclic doublet test input. Cut-off frequency f_c = 0.56 Hz.. Run R0201A.

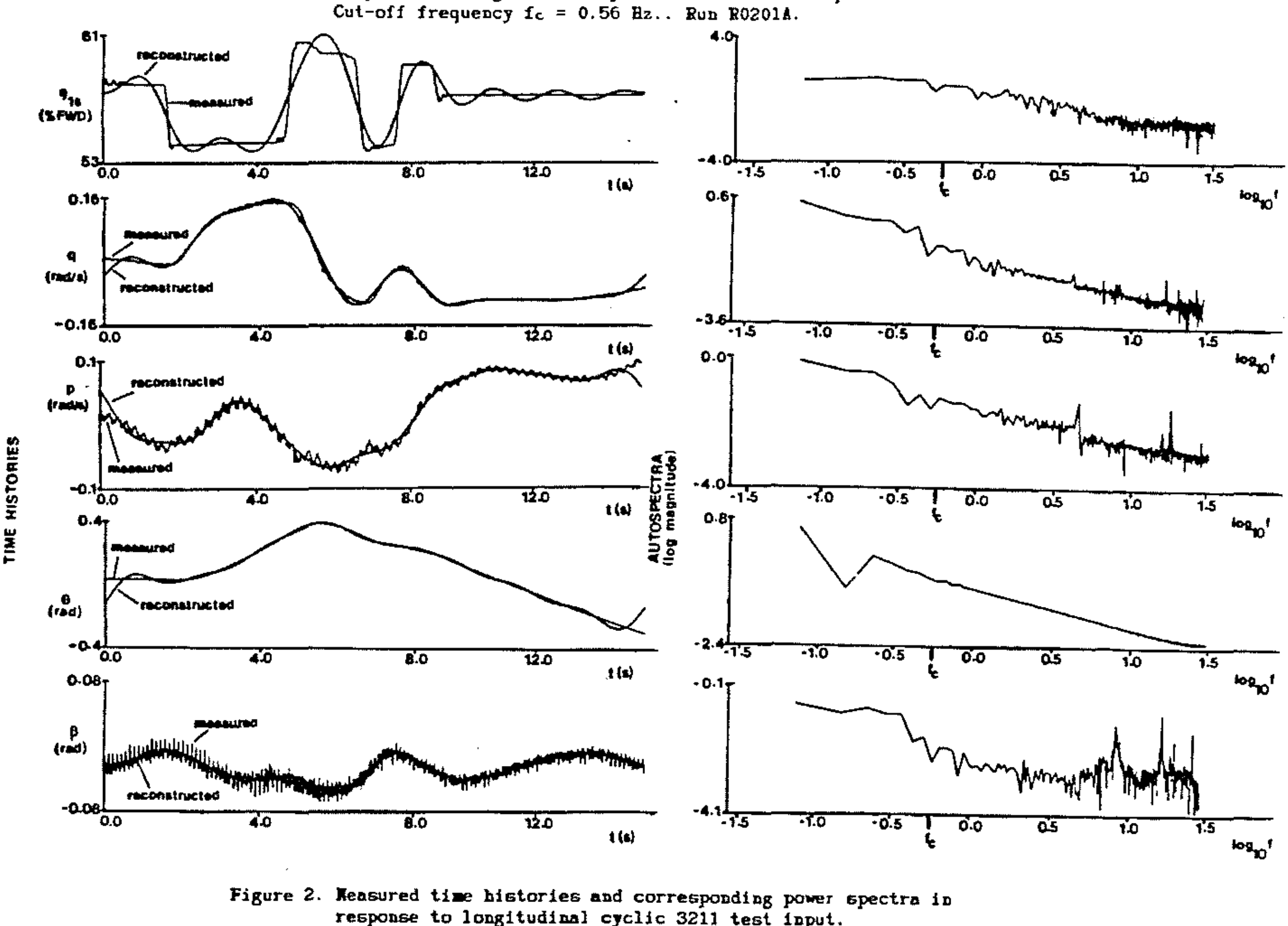

Figure 2. Measured time histories and corresponding power spectra in response to longitudinal cyclic 3211 test input. Cut-off frequency f_c = 0.56 Hz.. Run R0501A.

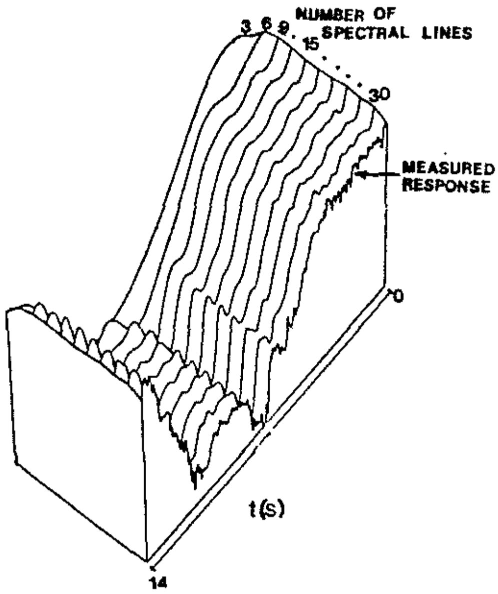

Figure 3. Forward velocity records in time-domain showing effect of number of spectral lines in frequency-domain representation. Run R0201A.

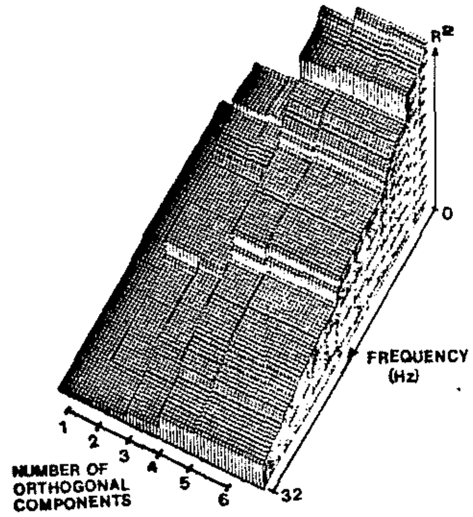

Figure 4. Dependence of squared correlation coefficient in identification of pitching moment equation on frequency range used and number of orthogonal components. Run R0201A.

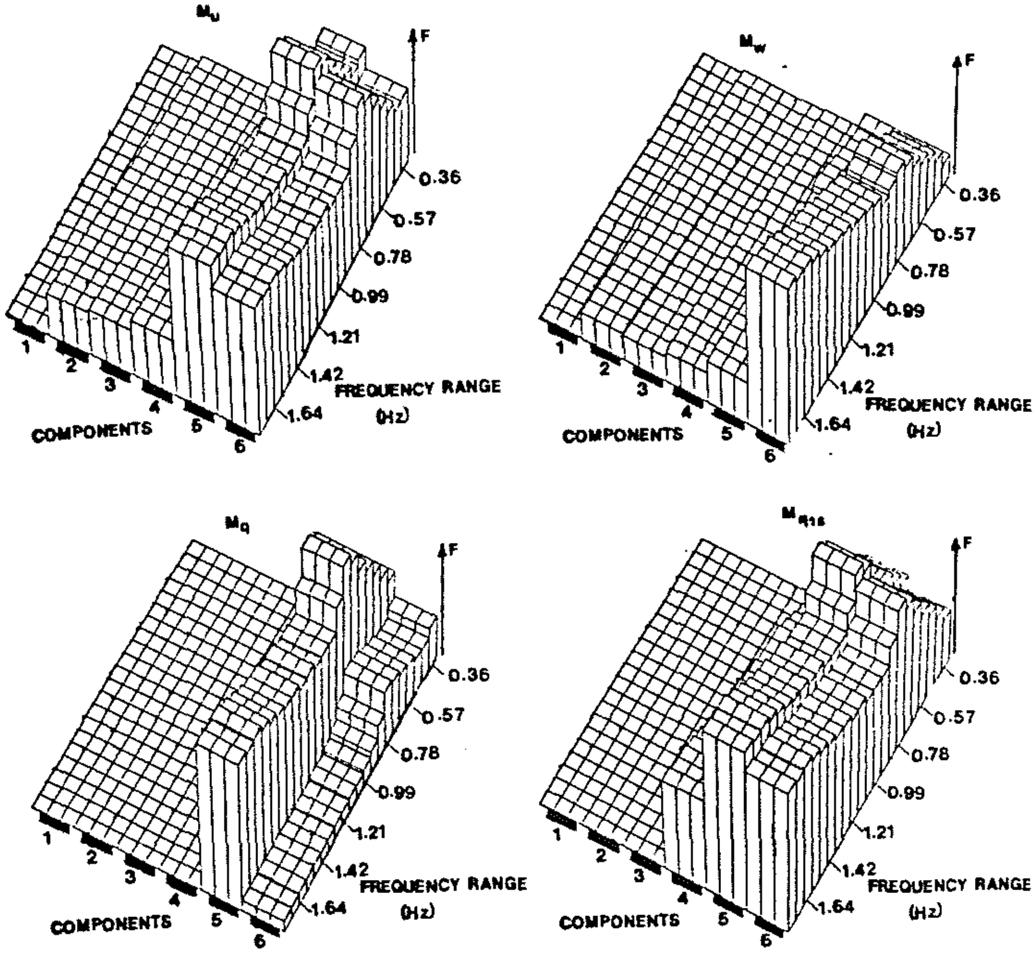

Figure 5. Partial F ratios for parameter estimates showing dependence upon frequency range and number of orthogonal components used. Run R0201A.

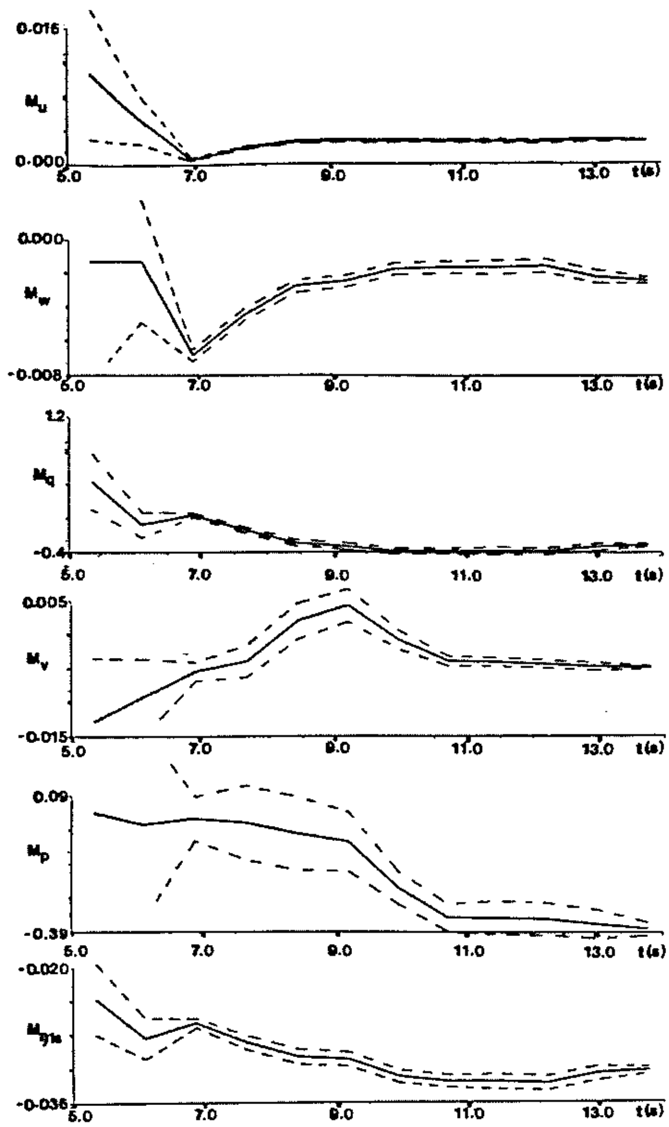

Figure 7. Variation of estimates with length of time-domain record. Run R0201A. Broken lines indicate 1 σ error bounds.

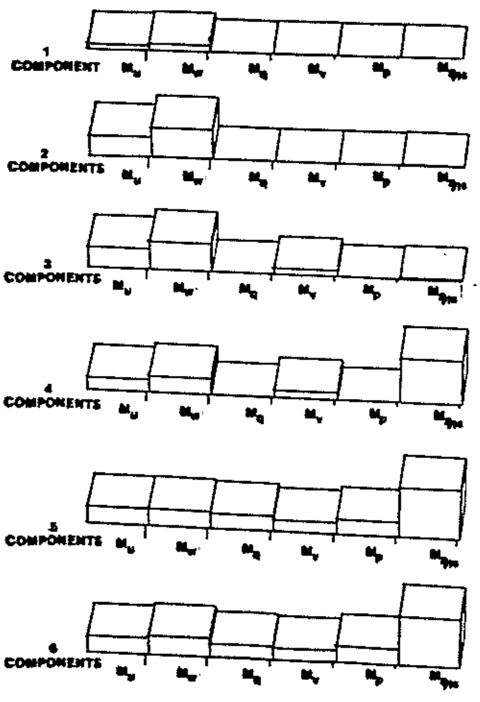

Figure 6. Parameter significance values, pitching moment equation. Run R0201A.

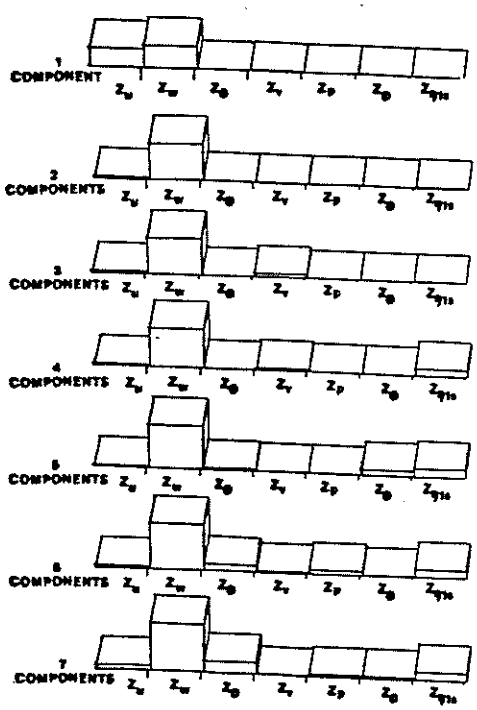

Figure 8. Parameter significance values, normal force equation. Run R0201A

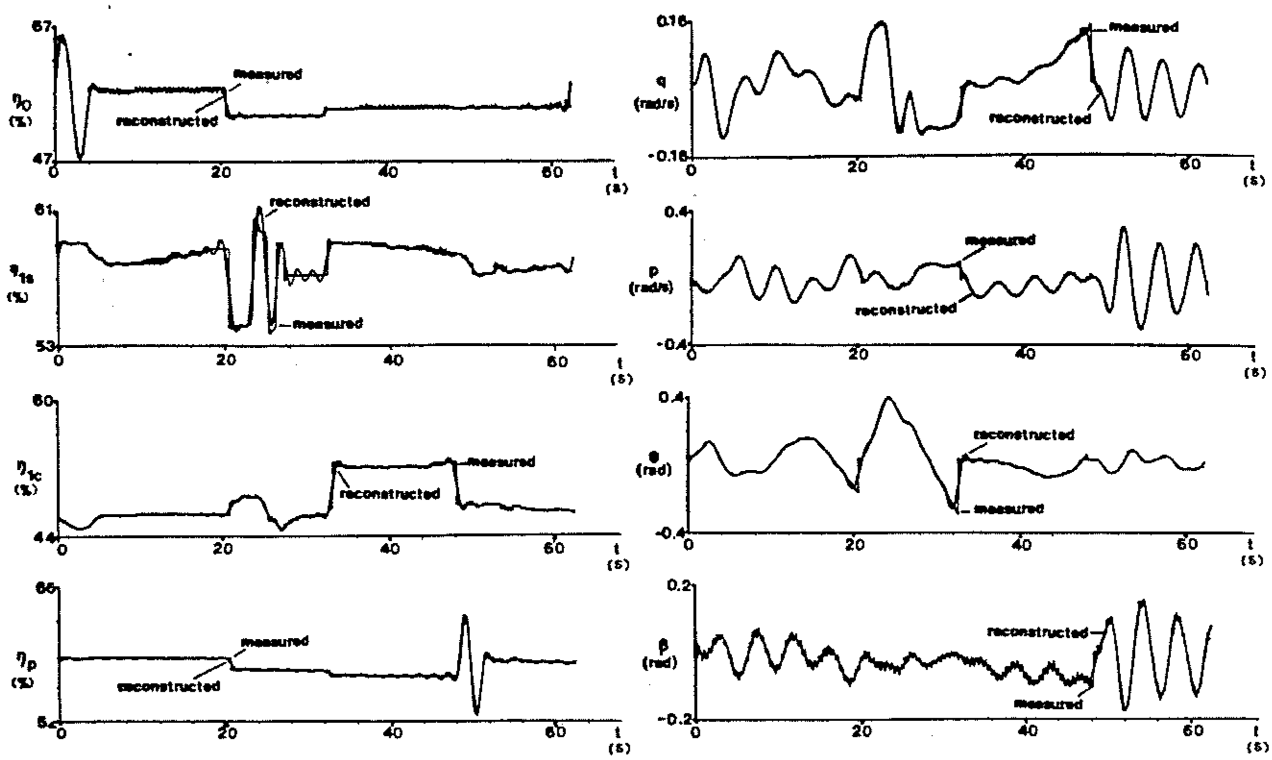

Figure 9. Multirun time-domain records with reconstructed records from frequency-domain superimposed (f_c = 0.56 Hz.).

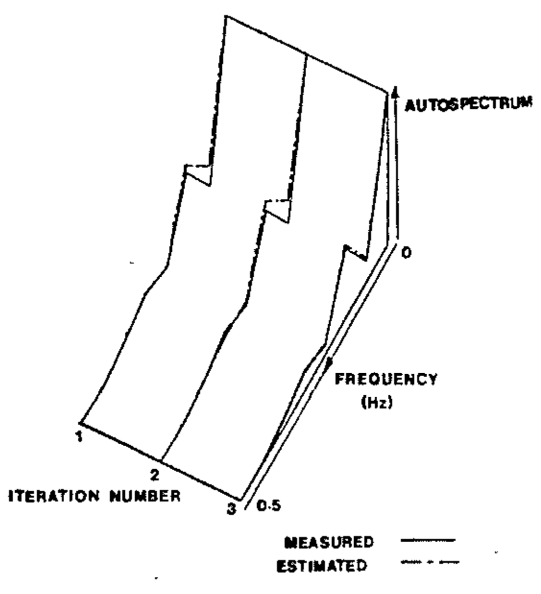

Figure 10. Convergence of incidence angle power spectra in output-error method.

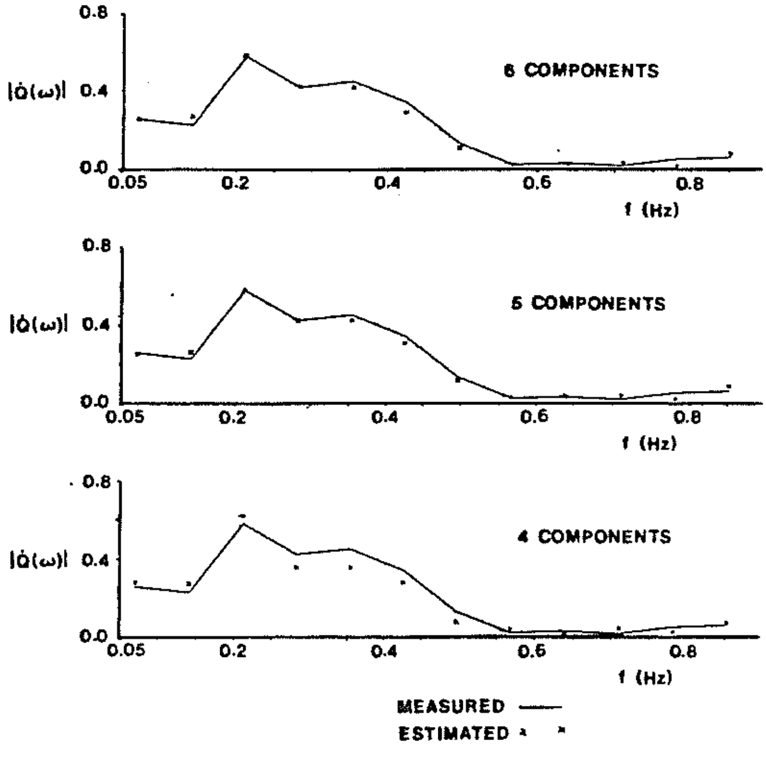

Figure 11a. Frequency-domain verification, pitching moment equation.

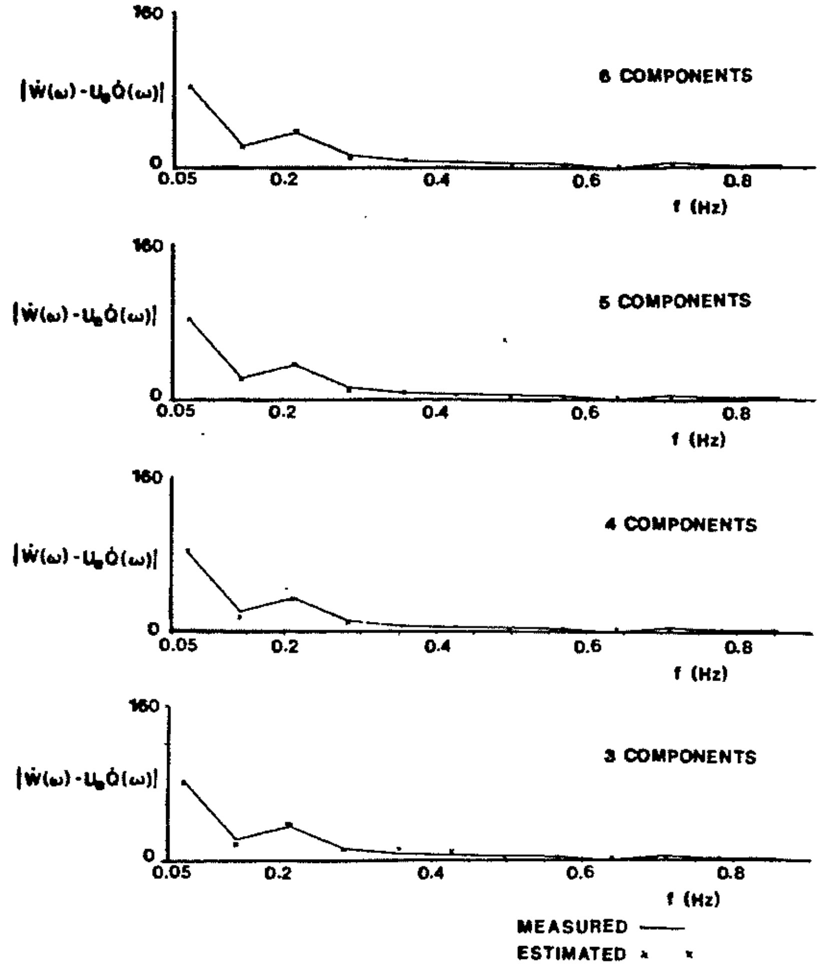

Figure 11b. Frequency-domain verification, normal force equation.

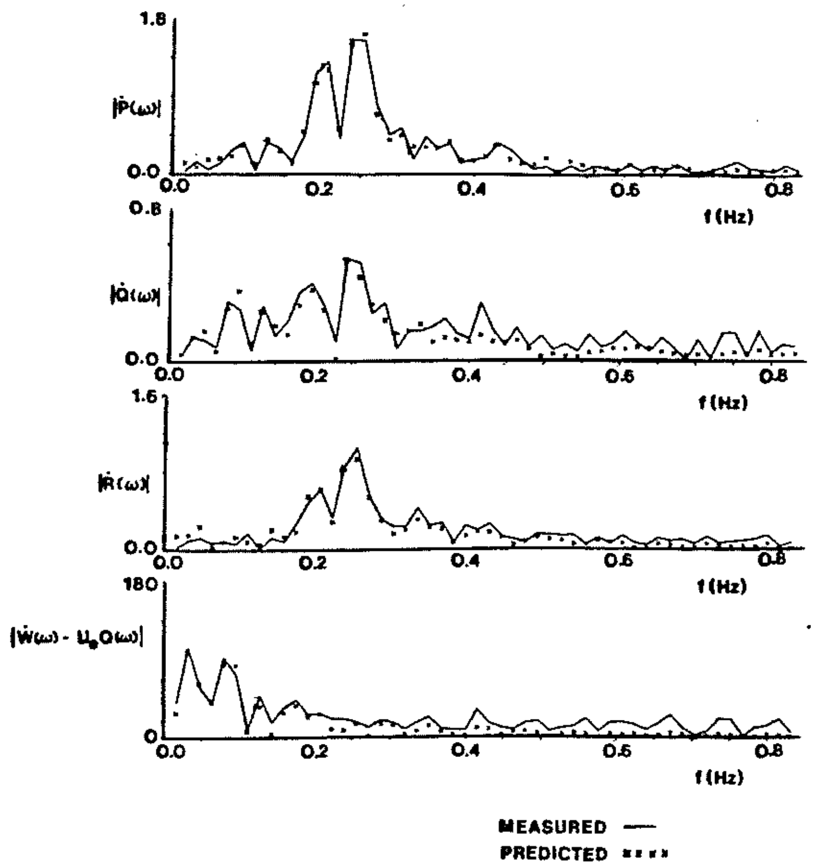

Figure 12. Frequency-domain verification, multirun case.

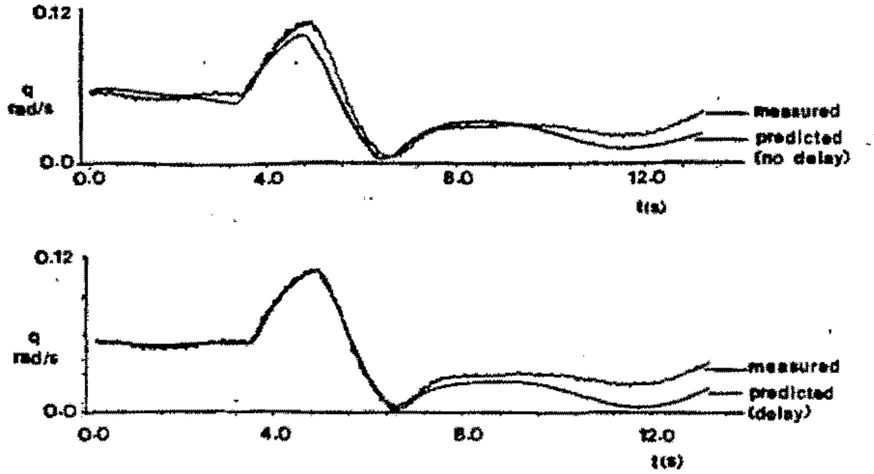

Figure 13. Time-domain verification, without and with time delay parameter.

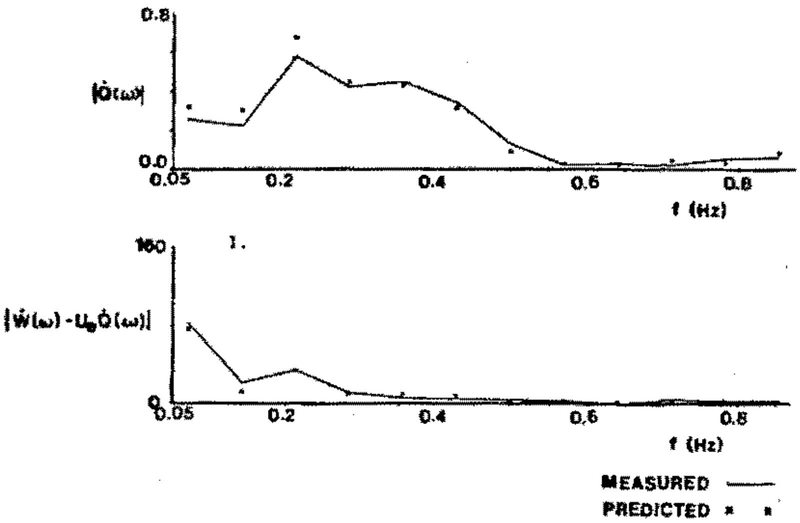

Figure 14a. Frequency-domain verification. Measured values obtained from response to longitudinal cyclic doublet. Predicted values based on model identified from multirun data.

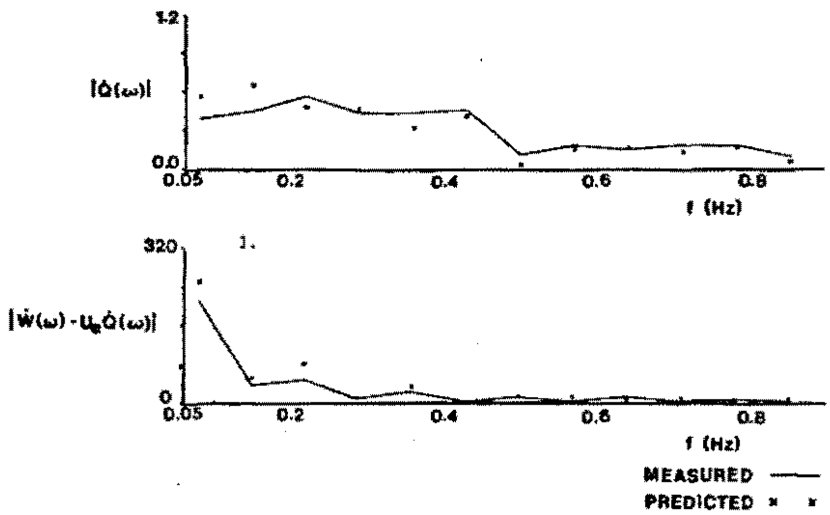

Figure 14b. Frequency-domain identification. Measured values obtained from response to longitudinal cyclic 3211 input. Predicted values based on model identified from response to longitudinal cyclic doublet input.

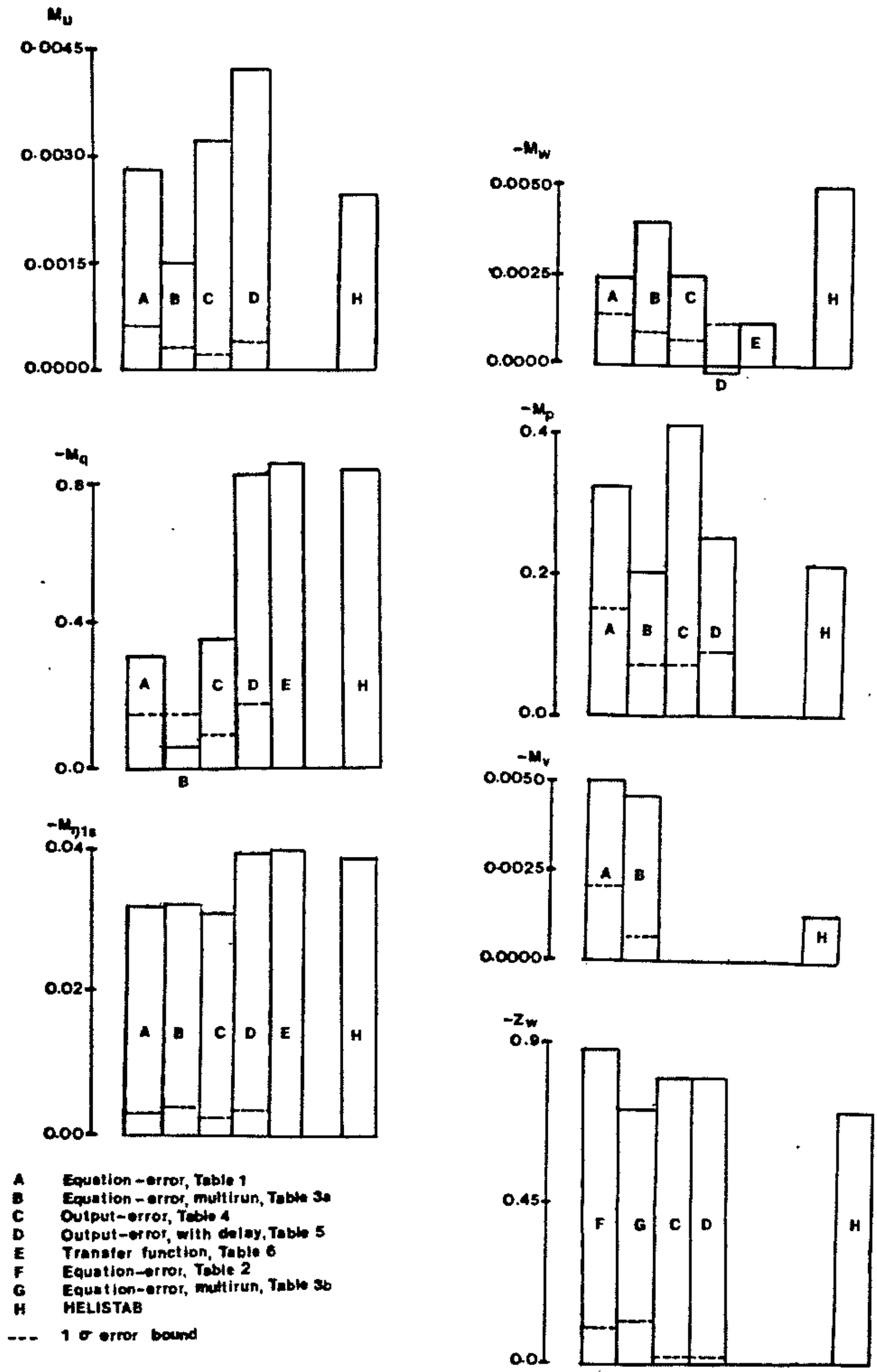

Figure 15. Parameter estimates obtained by 7 different methods used, together with HELISTAB values.